Maneuvering of the Space Station/Orbiter During an Assembly Flight

by

Paul A. Cooper
NASA Langley Research center

and

Alan E. Stockwell and Shih-Chin Wu
Lockheed Engineering & Sciences Company

Abstract

A large-angle, multi-body, dynamic modeling capability was developed to help validate numerical simulations of the dynamic motion and control forces which occur while berthing Space Station Freedom to the Shuttle Orbiter during early assembly flights. The paper describes the dynamics and control of the station, the attached Shuttle Remote Manipulator System, and the Orbiter during a maneuver from a gravity-gradient attitude to a torque equilibrium attitude using the station reaction control jets. The influence of the elastic behavior of the station and of the remote manipulator system on the attitude control of the station/Orbiter system during the maneuver is investigated. The flexibility of the station and the arm had only a minor influence on the attitude control of the system during the maneuver.

Introduction

Berthing of the Space Station Freedom (SSF) to the Orbiter is the primary method of mating the station to the Orbiter during initial assembly flights. The berthing procedure uses the Shuttle Remote Manipulator System (SRMS) to grapple the station and draw the station and Orbiter together.

A dynamic simulation of the berthing process is fairly complex, because it involves the interaction of large, highly-flexible components during a large motion maneuver while in orbit, where the components are subject to active control forces and gyroscopic, drag, and gravity-gradient forces and moments. The complexities of the station assembly numerical simulator are such that it was advisable to develop independently a comparable tool to help validate the simulator. This paper describes a large-angle, multi-body, dynamic modeling capability developed to help validate the SSF program numerical berthing simulator which will be used to analyze each assembly flight. These berthing simulations are used to calculate the dynamic motion and control forces that occur while berthing early-build configurations of Space Station Freedom to the Orbiter. During the early assembly flights, the station systems control the attitude of the combined spacecraft consisting of the Orbiter, SRMS and SSF. The combined spacecraft is herein referred to as the stack. The sixth assembly flight is the first flight that will use the station control systems rather than the Orbiter's Digital Auto Pilot (DAP) to maintain the attitude of the stack. On this flight and all subsequent assembly flights, the Orbiter reaction control jets are inhibited from firing once the SRMS has grappled the station. On the sixth assembly flight, the Orbiter carries the US laboratory module to the stage 5 station. Berthing during the sixth flight was selected as the validation simulation because the control systems of both the station and the SRMS are active during this maneuver.

The paper describes the salient features of each component of the system, including the reaction control system (RCS) for the SSF, the external loadings, the dimensions and masses and, where necessary, the structural dynamic representation. The procedure used to combine and integrate the dynamical equations governing the rigid-body dynamics, flexible-body modes, and control dynamics is described and simulation results for one maneuver are presented. The simulation is of a maneuver from a gravity-gradient (GG) attitude to a torque equilibrium attitude (TEA) using station RCS jets with the brakes applied at each SRMS joint.

Description of Maneuver Simulated

The simulation is concerned with the berthing maneuver during the sixth assembly flight, after the SRMS has grappled the stage 5 station. The stage 5 station configuration is shown in figure 1. The solar alpha rotary joint permits a relative rotation of the photovoltaic (PV) arrays with respect to the core body so that the attitude of the inner portion can be held constant during an orbit while the PV arrays track the sun and provide electrical power. Before the berthing maneuver begins, the arrays are rotated to a position which will minimize plume loads from the Orbiter jets during the final approach of the Orbiter before

grappling occurs. The PV joints are then locked and remain locked during the entire berthing maneuver. Figure 1 also indicates the location of the avionics platform containing sensors which provide attitude and attitude rate information. The attitude can be controlled by firing jets, located on the top and bottom of the inboard station framework, at a constant force level of 25 lbs per jet, or by a set of four double-gimbaled control moment gyro's (CMG's) located on a platform close to the avionics platform. As indicated in figure 2, The Orbiter approaches the station along the direction opposite the orbital velocity vector and flies in tandem with the station maintaining a distance of about 30 feet between the V-guides in the cargo bay and the trunnion pins on the docking adapter. The SRMS end effector moves from its berth on the port side of the cargo bay toward the station and grapples the station by snaring the grapple fixture located on the resource node, a pressurized shell attached to the station framework inboard of the alpha joint.

The simulation performed in the current study begins after the SRMS has grappled the resource node and attitude control has been handed over to the station. The brakes are applied to each of the SRMS joints and the RCS jets are fired to move the station from a GG attitude to a computed TEA. The torque equilibrium attitude is defined as the average attitude which must be held so that no net angular momentum is accumulated over an orbit in the presence of gravity-gradient, aerodynamic, and orbital gyroscopic disturbances. Figure 3 contains a schematic drawing of the stack configuration before and after the maneuver.

To complete the berthing, the brakes on the SRMS are released and the station RCS jets are inhibited from firing. The attitude of the stack is now maintained by the station CMG momentum management system and berthing begins as the joint motors on the SRMS are used to draw the station and the Orbiter together. The TEA changes during the berthing, since the inertia of the stack changes. Results from a simulation of this final maneuver are not presented but are discussed in reference 1.

SSF/Orbiter Dimensions and Masses

Figure 4 shows the relative size and location of the stage 5 station, the Orbiter, and the extended SRMS at the beginning of the simulation. The SSF has a weight of 145,000 lbs and the Orbiter, with the lab module in the cargo bay, has a weight of 250,000 lbs. The SRMS has a weight of only 1,000 lbs. The distance from the base of the SRMS to the grapple point is 45.3 feet.

Space Station Freedom

The finite element model of SSF, briefly described here, is documented in detail in the SSF Preliminary Design Review (PDR) Loads Data Book of reference 2. The MSC/NASTRAN model , shown in figure 5, consisted of ten internal superelements and three external superelements. Each segment of the pre-integrated truss (PIT) was grouped as a superelement as were other major components such as the Solar Alpha Rotary Joint (SARJ) and the Pressurized

Docking Adapter (PDA). The PV arrays and the electrical power system (EPS) radiator were supplied as Craig-Bampton modal models (external superelements). Limited geometry and data-recovery information was supplied along with the reduced mass and stiffness matrices and the component-mode eigenvectors. Customized DMAP Alters[3] were used to process the external superelement information and store it in a database. The only alteration made to the model was the addition of a grid point to represent the grapple fixture located on the outer shell of the resource node. The SRMS captures the station by latching on to it at this point. The SSF model was constrained in all six DOF at the grapple fixture in order to incorporate it as a flexible component in the multi-body simulation.

The model consisted of almost 15,000 (G-set) degrees of freedom (DOF), however component mode reduction was applied to each of the internal superelements[2] and the final A-set size of the eigenvalue problem was reduced to 781 DOF. Mode shapes and frequencies up to 5Hz were calculated using the Lanczos method. The space station structural dynamics are represented during the TEA simulation by a set of 36 natural modes which range in frequency from 0.1 Hz to close to five Hz. The modes were selected to provide an accurate representation of the flexible response at the station sensor location caused by forces applied at the RCS jet locations. The modes were obtained for the model fixed at the grapple fixture point. Three of the modes retained for the multi-body dynamic analysis are shown in figure 6.

Shuttle Remote Manipulator System

The Shuttle Remote Manipulator System[4], shown in figure 7, is a six-joint anthropomorphic mechanical arm originally designed to deploy payloads up to 65,000 lbs. The arm has a length of 50 ft. 3 in. and a diameter of 15 in. Each of the six arm joints is a revolute joint whose position is controlled by a servo motor with an encoder to give joint position and a tachometer to give joint rate. The TEA simulation uses a motor-brake system, which allows the joints to slip when friction levels are exceeded to prevent overloading of the arm. For the simulation of the elastic behavior of the SRMS, the upper and lower arms were modeled with prismatic beam (CBAR) elements. Each "link" was modeled using nine elements. This discretization provided a close approximation of the overall mass properties of each link. Cantilever boundary conditions were used to calculate the modes for inclusion in the multi-body simulation. The two lowest frequencies of each arm were the first-bending frequencies in the two orthogonal bending directions. The first two frequencies of the lower arm were 4.5 Hz and 4.9 Hz, and the frequencies of the upper arm were 5.1 Hz and 5.2 Hz. All other links between joints were treated as rigid bodies.

RCS control system

A simplified block diagram of the RCS control system is shown in figure 8. The attitude determination system (ADS) measures the attitude and feeds this information back to the controller. The control system is designed for use in all configurations of the station covering a large range of inertias during the 3-year

assembly process. To accommodate this wide range of system parameters, a mass estimator is provided to determine the on-orbit inertias and to adjust the control gains to provide acceptable performance. There are two bending filters (low pass filters designed to remove higher frequency components of the feedback position and rate signals) which are not shown in the block diagram of figure 8.

Simulation Procedures

The multi-body analysis computes the relative motion of nine distinct bodies as shown in figure 9. Each joint connecting the nine arm components has a friction model which will allow the brakes to slip at a given applied moment. Figure 10 contains a block diagram describing the simulation architecture. The time integration of the set of dynamical differential equations, including the control equations, was originally to be performed using a commercial code called Dynamic Analysis and Design Systems, DADS[5]; however, the integration schemes in DADS limit the integration to either single sampling rate control systems or multi-rate systems where the rates are multiples of a single rate. The SSF and SRMS control systems use several different unrelated sampling rates. All control equations were available as FORTRAN code and were programmed external to the DADS program as was the time-integration algorithm, a 3rd-order Adams-Bashforth procedure. The DADS code was called as a subroutine with control loads supplied at constant time steps from the controls routine. The loads were computed in the controls subroutine external to DADS using appropriate integration procedures consistent with the various control sampling rates. The aerodynamic and gravity-gradient moments, which are also computed external to DADS, and the control loads are applied as input at center of mass locations, SRMS joints, and SSF controller locations as appropriate.

The orbital environmental disturbances including the gravity-gradient moments and the aerodynamic moments were computed as external loads. The computed gravity-gradient moment is applied as a rigid-body moment about the stack center of mass. The TEA was computed for the given configuration by minimizing the momentum which must be absorbed by a perfect controller to maintain a constant attitude through one complete orbit. A code called IDEAS**2 was used to compute the TEA[6]. The initial TEA before berthing begins is expressed as a pitch-yaw-roll Euler sequence describing the relative orientation of the station with respect to a non-inertial orbital coordinate system.

Incorporating the FE Model in DADS

The DADS multi-body dynamics code uses two sets of generalized coordinates to formulate the equations of motion for a flexible body. The position and rotation of a body reference frame represent the rigid-body motion, and the modal coordinates represent the small-deformation elastic motion. The development of the equations of motion is summarized in Appendix A. The standard DADS/NASTRAN interface requires a single MSC/NASTRAN run to generate the geometry, mass and stiffness matrices, and mode shapes and frequencies of the flexible body. The DADS Intermediate Processor (IP) converts this information

into standard DADS flexible-body input data, however the DADS IP was not set up to handle structures composed of multiple superelements. Therefore, the standard procedure for adding flexibility to a body had to be modified to allow processing of the external superelements (PV arrays and IEA radiator). The DADS program assumes a lumped mass formulation for the flexible body and requires each grid point in the body to have a mass associated with it. The lumped mass matrix is then used to calculate nonlinear terms in the equations of motion. Since the detailed mass distribution was not available for the external superelements, an approximate mass representation was generated for the grid points which were used to graphically represent the geometry of the PV arrays and EPS radiator in the assembled finite element model. Superelement cards (e.g., SESET) were removed from the bulk data, and the approximate external superelement mass data was combined with the mass data for the physical portions of the SC-5 model to produce a single mass matrix for the SSF. The superelement mode shapes calculated using component mode synthesis were combined into "system" mode shapes with the aid of a program called Semcomb, developed by the Structural Dynamics Research Corporation, and the data was combined with the mass and geometry data using a customized DMAP procedure to format the data for the DADS Intermediate Processor (IP). Figure 11 summarizes the procedure used to generate the DADS flexible-body input.

Simulation Results for TEA Maneuver

The TEA maneuver required an attitude change from a gravity-gradient position, as shown in figure 3, to an attitude orientation of pitch, yaw and roll of -22.1°, -7.4° and 3°, respectively. The resulting attitude-change time history is shown in figure 12. The time integration was performed with a time step of 0.001 seconds and the computations took approximately 72 hours of dedicated CPU time on an SGI 4D/440 workstation. The station structural dynamics were represented using 36 normal modes. A simulation using a ten-mode model was also computed and compared to the 36-mode simulation. The response differences were within the accuracy of the computation and thus the ten-mode model was deemed to be sufficient in representing the dynamics of the station in future investigations. A conservative proportional damping level of 0.2 percent of critical damping was assumed for each mode. The actual jet firing times, shown in figure 13, occur as pulses of between approximately 0.2 and 1 second duration. The jets are inhibited from firing more often than once every 33 seconds to reduce structural dynamic response.

The jet firing times, i.e., the total time that the jets were firing during the simulation time, were compared for the simulation with flexible components and a corresponding simulation where all components were assumed to be rigid. The firing time was 7-percent greater for the simulation with a flexible SSF and SRMS. This amounted to an increase of about four seconds of firing during the 2500-second simulation and was deemed negligible. When the bending filter in the SSF control system was removed for the simulation with flexible components, the amount of firing time only increased by an additional two seconds.

The SRMS joints were slightly overloaded when the jets were fired and each wrist joint exhibited some slippage during the first 750 seconds of the simulation. The Point Of Resolution motion (POR) is plotted in figure 14 and shows the total absolute motion of the end effector of the SRMS with respect to the Orbiter with the brakes engaged. The motion is composed of slip in the wrist joints, and the accumulated freeplay and flexibility in the drive train for all joints. The pulsing of the jets causes a build-up of motion during the first 500 seconds of the simulation. As an example of the flexible effects, the motion of the tip of a PV array was calculated using MSC/NASTRAN to perform an open-loop transient analysis. Forces and moments at the grapple fixture and jet-firing time-histories were recovered from the multi-body simulation and converted to MSC/NASTRAN dynamic load input. A conservative modal damping value of 0.2 percent critical damping was assumed for all modes. The PV tip motion, plotted in figure 15, has a maximum displacement to one side of 2.8 inches. This is a minor displacement when considering that the PV array is over 1300 inches long. Loads at the root of the array were inspected and were well below the allowable load.

Concluding Remarks

A large-angle, multi-body, dynamic modeling capability was developed to help validate numerical simulations of the dynamic motion and control forces which occur while berthing early-build configurations of Space Station Freedom to the Shuttle Orbiter during assembly flights. The paper describes the dynamics and control of the station, the attached Shuttle Remote Manipulator System, and the Shuttle Orbiter during a maneuver from a gravity-gradient configuration to a torque equilibrium configuration, using station reaction control jets, and then during the subsequent berthing of the station to the Orbiter with the station control moment gyros actively maintaining attitude. The influence of the elastic behavior of the station and of the remote manipulator system on the attitude control of the station/Orbiter system during the maneuvers was investigated and found to have only a minor influence on the attitude control of the system during the maneuvers.

References

1. Cooper, P.A., et. al., "Simulation of the Assembly Dynamics and Control of Space Station Freedom," to be presented at the AIAA Guidance, Navigation and Control Conference, August 9-11, 1993.

2. "SSFP PDR Loads Data Book, Volume II: On Orbit Loads," NASA SSJ 10450, September 15, 1991.

3. Shein, S.-L., Marquette, B., and Rose, T., "Superelement Technology Application and Development in Dynamic Analysis of Large Space Structures," Proceedings of the 1991 MSC World User's Conference, March 11-15, 1991.

4. "Payload Deployment and Retrieval System Simulation Database, Version 1.0, RMS Operations," NASA JSC-25134, July 1, 1991.

5. *DADS User's Manual*, Rev. 6.5 , CADSI, March 1991.

6. "SSF Program IDEAS**2 Users Guide (Version SSP 2.0)", SSE-E-88-R24 Grumman Space Systems, Oct 31, 1988.

7. Wu, S. C., Haug, E. J. and Kim, S. S.,"A Variational Approach to Dynamics of Flexible Multi-body Systems", Mechanics of Structures and Machines, 17(1), pp. 3-32, 1989.

Appendix A - Equations of Motion of Flexible Multi-body Systems

In order to specify the configuration of a deformable body, it is necessary to define a set of generalized coordinates that uniquely define the global position and orientation of every point in the body. Consider the deformable body in an inertial x-y-z frame, as shown in Fig. A-1. An x'-y'-z' body reference

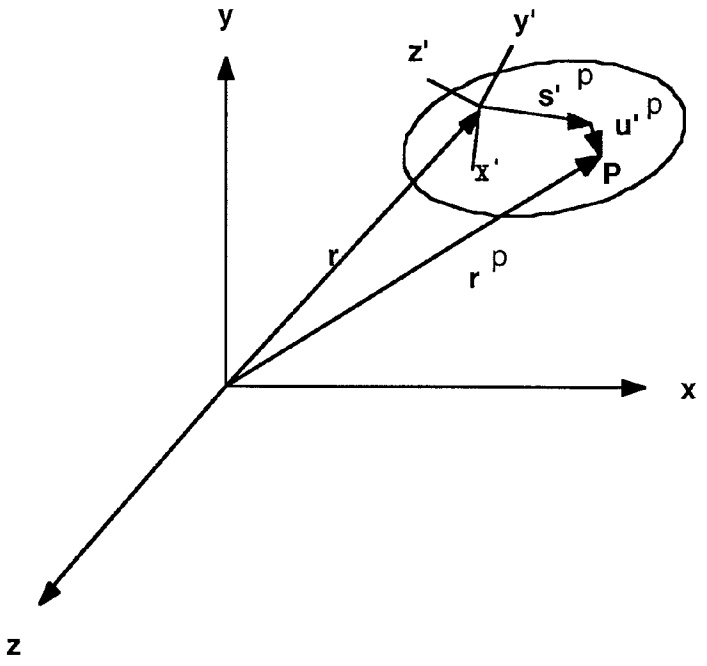

Figure A-1 Reference generalized coordinates

frame is chosen to locate and orient the body in the inertia frame. Vector **r** from the origin of the x-y-z frame to the origin of the x'-y'-z' body reference frame defines the global position of the body reference frame. Euler Parameters are used as generalized coordinates to define the orientation of the body reference frame relative to the inertial frame.

Using a finite element model, the body is discretized into a large number of elements that are connected at their nodes. The mass of each element is distributed to nodes of the element, using standard finite element lumped mass approximations. The position vector of a typical point P on the body can thus be written as

$$\mathbf{r}^P = \mathbf{r} + \mathbf{A}(\mathbf{s}'^P + \mathbf{u}'^P) \tag{1}$$

where **A** is the orthogonal transformation matrix from the x'-y'-z' frame to the x-y-z frame, $\mathbf{s}'^P$ is the position vector of point P in the x'-y'-z' frame before the body is deformed, and $\mathbf{u}'^P$ is the displacement of point P relative to x'-y'-z' frame due to deformation.

To reduce the number of elastic deformation coordinates, a Ritz approximation is employed. By defining a set of deformation modes of the body, the displacement field can be represented as a linear combination of deformation modes; i.e.,

$$\mathbf{u}' = \sum_{i=1}^{k} \Psi_i a_i \tag{2}$$

where Ψ_i is a 6Nx1 vector of nodal displacements that defines the ith deformation mode and a_i is the associated modal coordinate, N is the number of nodes in the finite element model, k is the number of modal coordinates, and **u'** contains both nodal displacements and rotations. Ψ_i must contain no rigid body motion. In matrix form, Eq. 2 is written as

$$\mathbf{u}' = \Psi \mathbf{a}$$

where

$$\Psi = [\psi_1, \ \psi_2, \ \ldots, \ \psi_k]$$

is the modal matrix and

$$\mathbf{a} = [a_1, \ a_2, \ \ldots, \ a_k]^T$$

is the modal coordinate vector. Displacement due to Deformation at point P is

$$\mathbf{u}'^P = \Psi^P \mathbf{a} \tag{3}$$

where Ψ^P is the translational deformation modal submatrix at point P.

Substituting Eqs. 3 into Eq.1, the position vector of point P in the inertial frame can be written as

$$\mathbf{r}^P = \mathbf{r} + \mathbf{A}(\mathbf{s}'^P + \Psi^P \mathbf{a}) \equiv \mathbf{r} + \mathbf{A}\rho'^P \tag{4}$$

where

$$\rho'^P \equiv \mathbf{s}'^P + \Psi^P \mathbf{a} \tag{5}$$

In summary, in order to uniquely specify the state of a flexible component, two sets of generalized coordinates are employed. The first set consists of generalized coordinates of a body reference frame that is chosen to define the location and orientation of the body in the inertial frame. The second set consists of modal coordinates that characterize elastic deformation.

With the kinematics of an arbitrary point in a flexible body defined in Eq. 4, the variational equations of motion of a body can be formally derived using virtual work theory. The equations of motion for the system are obtained as a set of ordinary differential equations in the following general forms:

$$\mathbf{M}(\mathbf{q})\ddot{\mathbf{q}} = \mathbf{Q}(\mathbf{q}, \dot{\mathbf{q}}) + \mathbf{f} \tag{6}$$

where $\mathbf{q}$ is the system generalized coordinates vector which includes rigid body degrees-of-freedom of the system and modal coordinates of each flexible component, $\dot{\mathbf{q}}$, and $\ddot{\mathbf{q}}$ are time derivatives, and twice time derivatives of $\mathbf{q}$, respectively, and **M** is the generalized mass matrix of the system, **Q** is the vector of centripetal and Coriolis forces, and **f** is the vector of external forces. Detailed derivations and expressions of Eq. 6 are given in Reference 7.

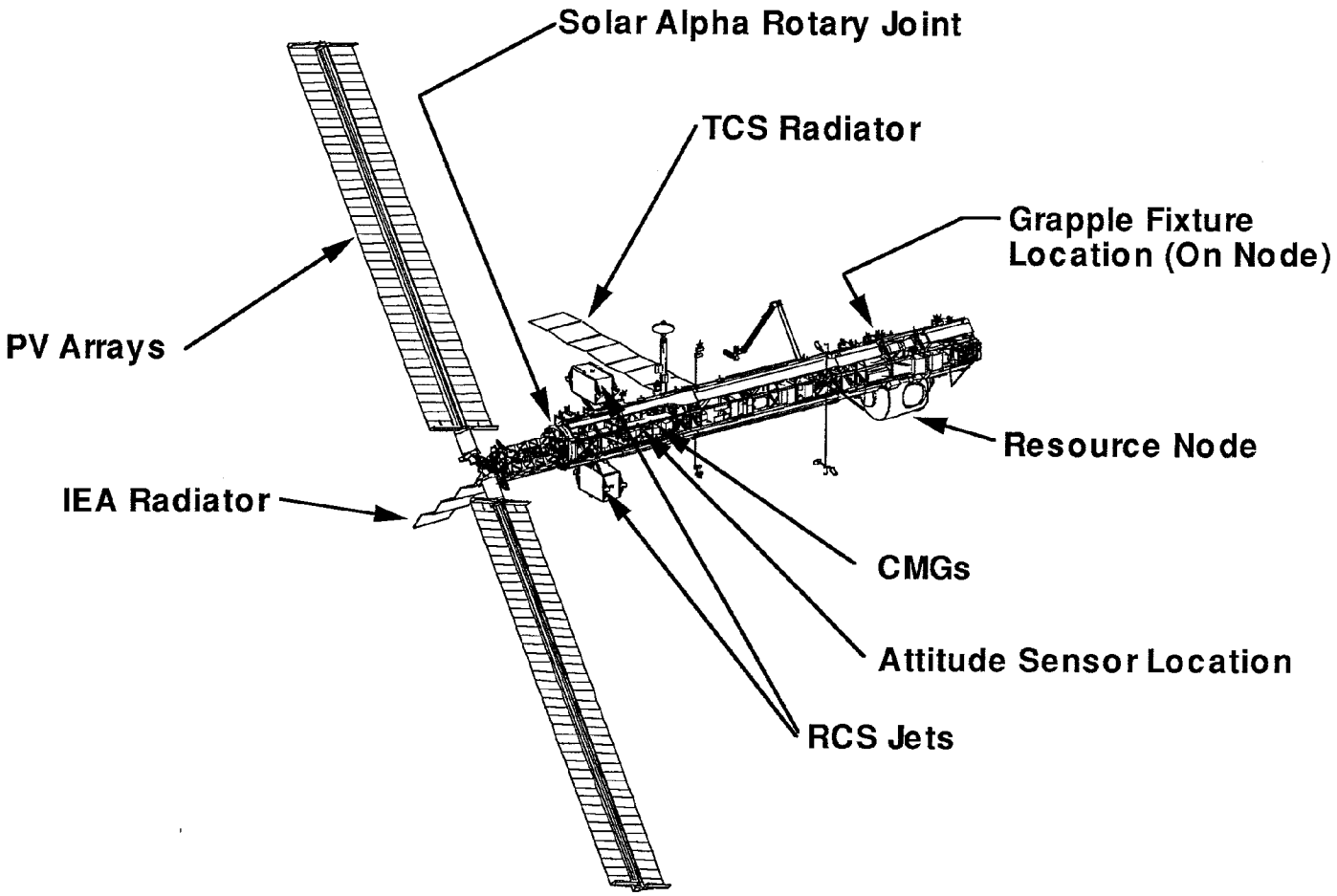

Figure 1 Space Station Freedom - Stage 5

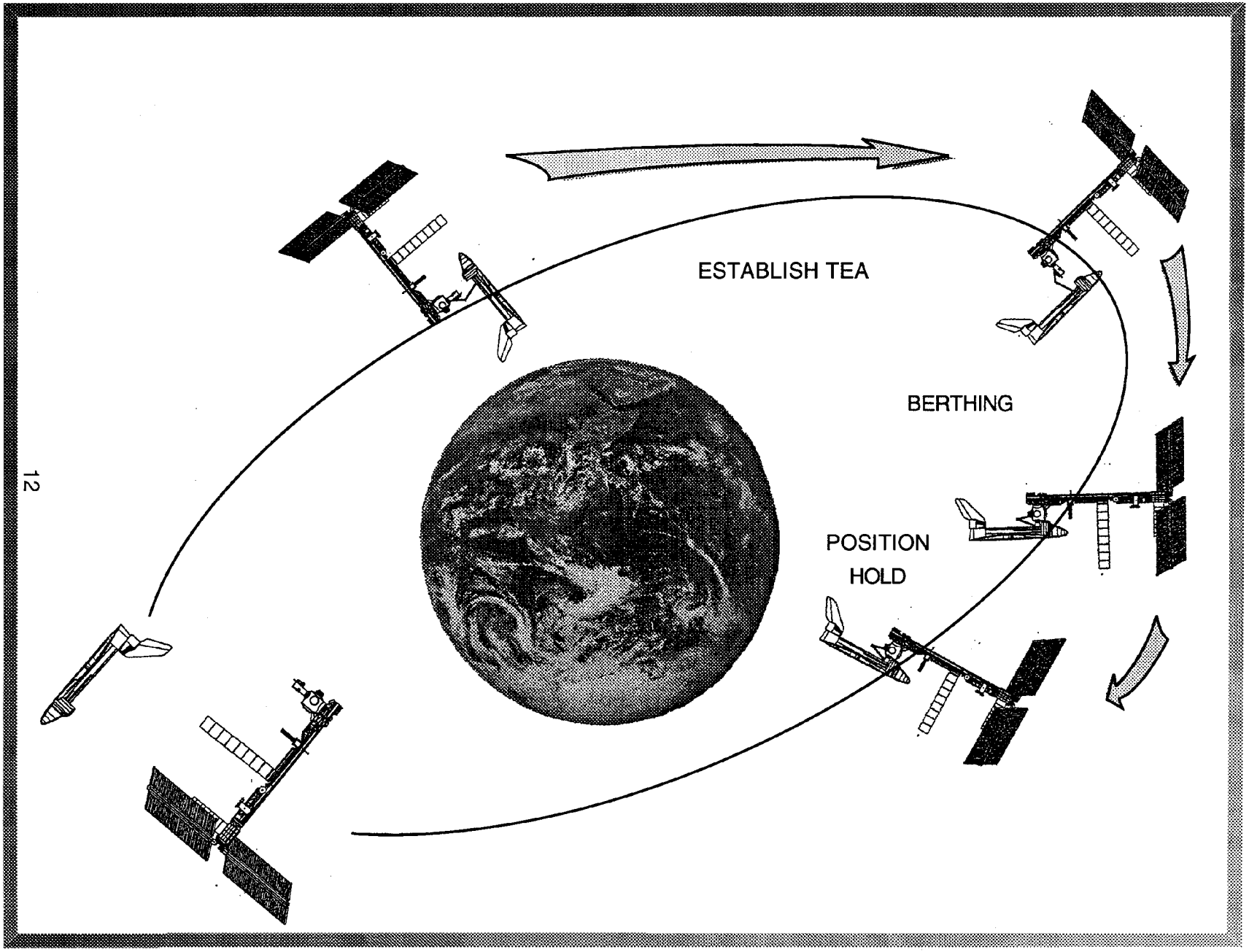

Figure 2 TEA/Berthing simulation

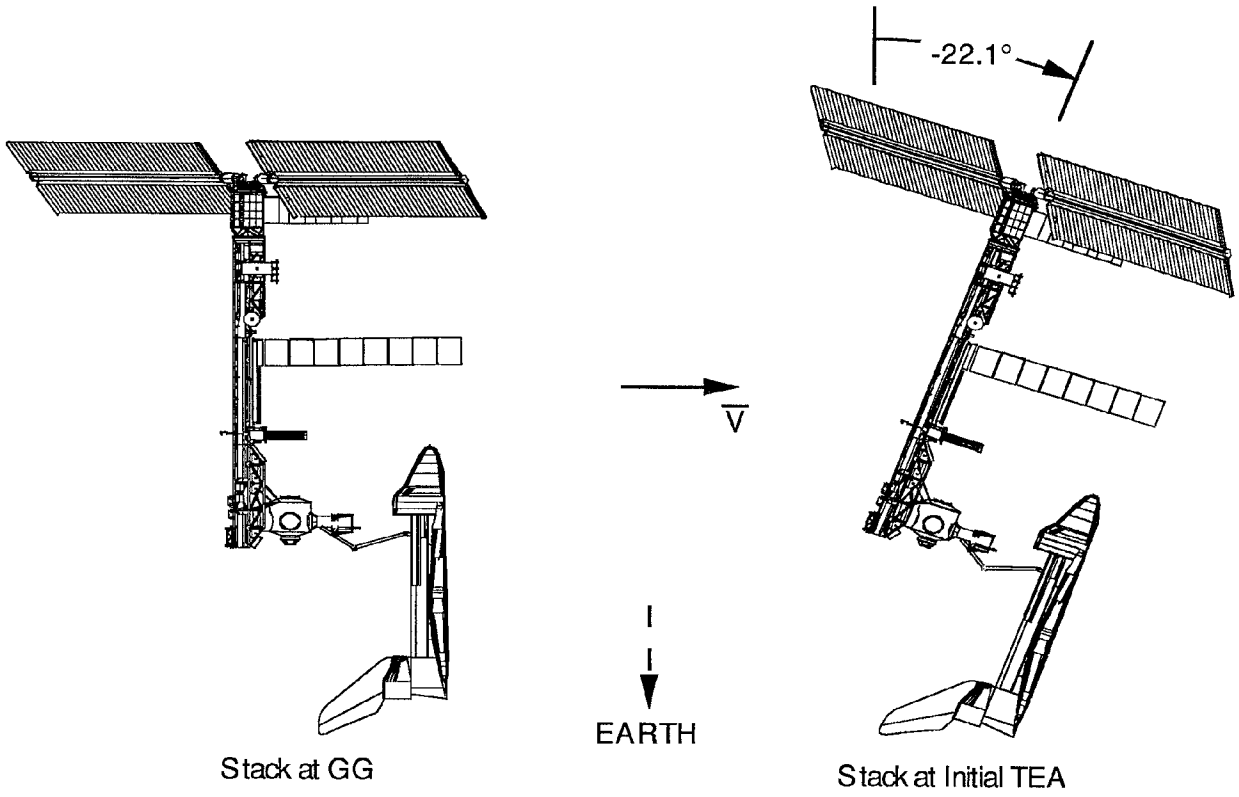

Figure 3 Establishment of initial torque equilibrium attitude (TEA)

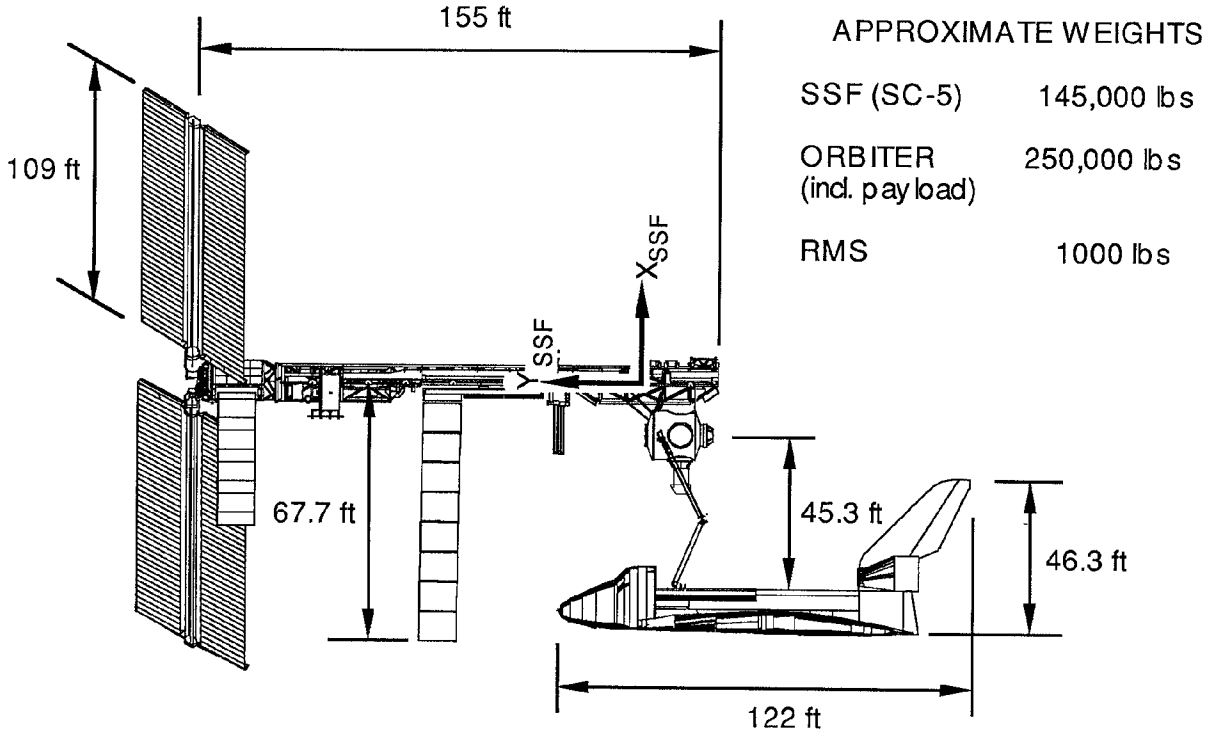

Figure 4 SSF/Orbiter approximate dimensions, flight MB-6, orbiter berthed to SC-5 station

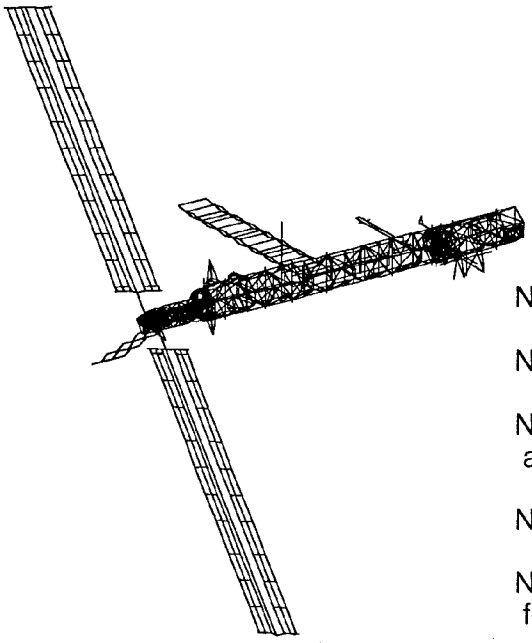

Number of Grid Points	= 2442
Number of Elements	= 2851
Number of Dynamic DOF after component mode reduction	= 781
Number of Modes < 5 Hz	= 181
Number of key modes selected for simulation	= 36

Figure 5 SC-5 finite element model

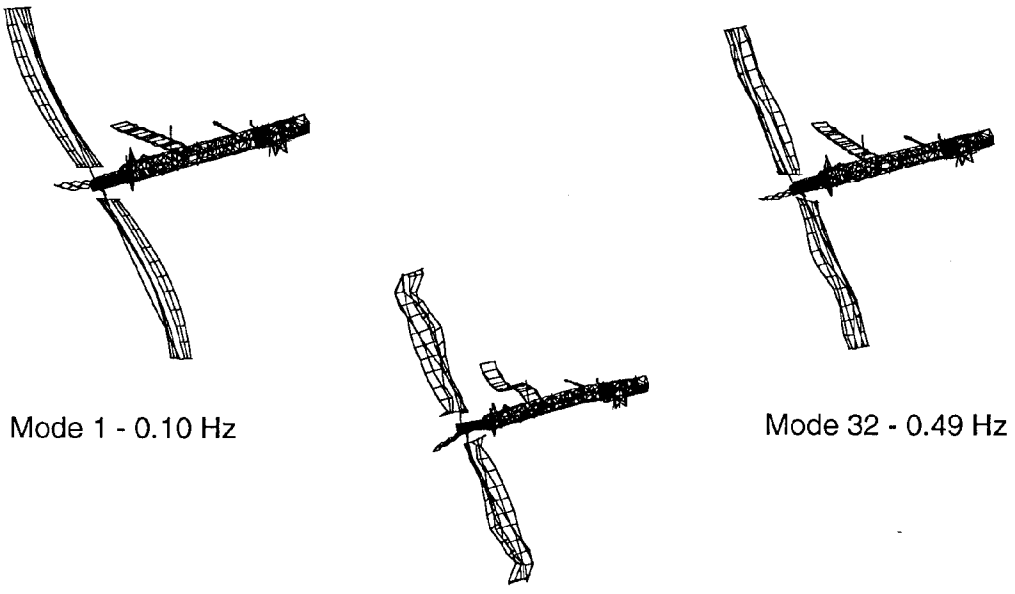

Figure 6 Selected flexible modes affecting rotation and rotation-rate sensors

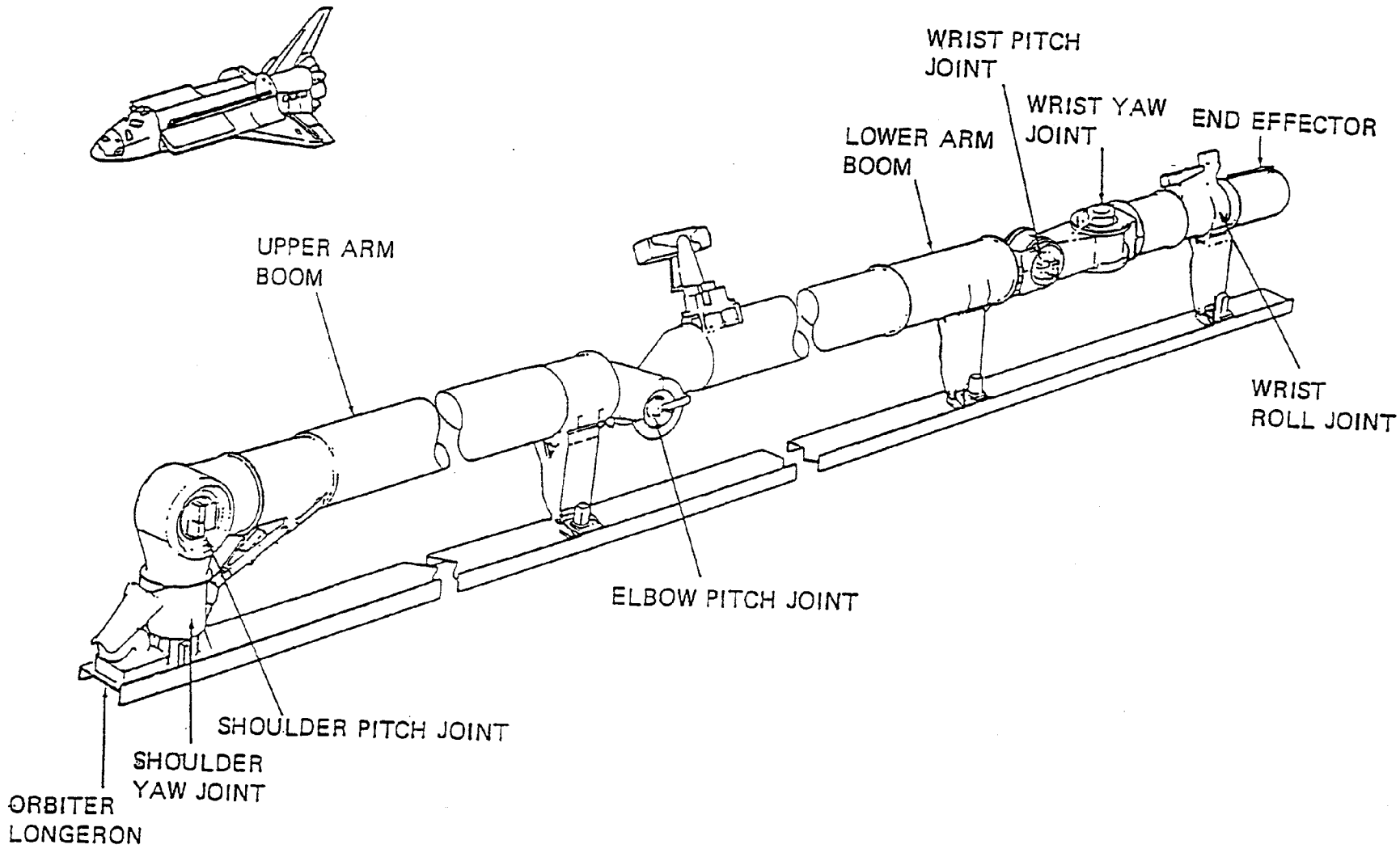

Figure 7 Shuttle Remote Manipulator System

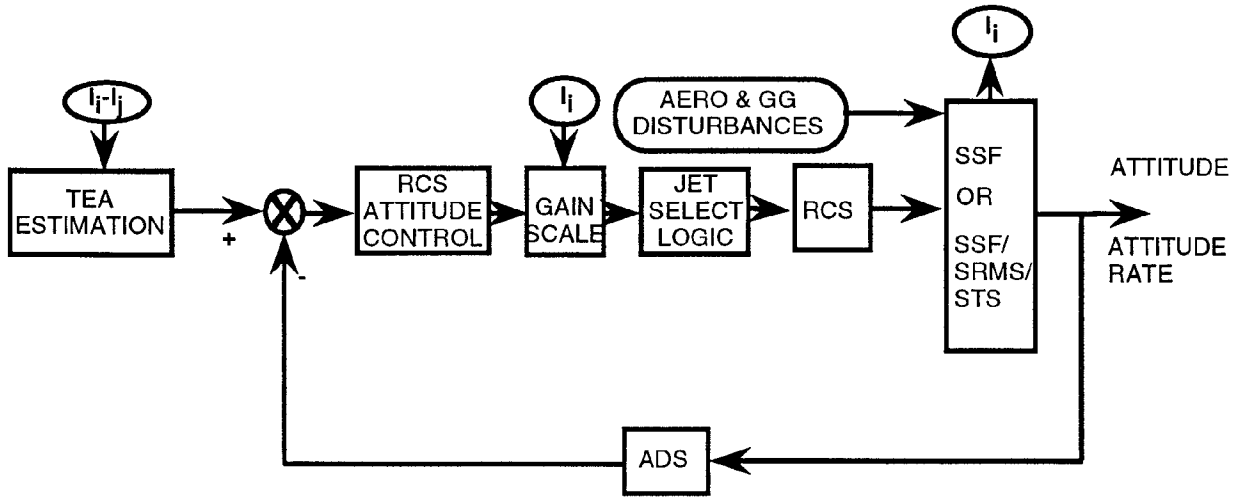

Figure 8 SSF RCS attitude controller

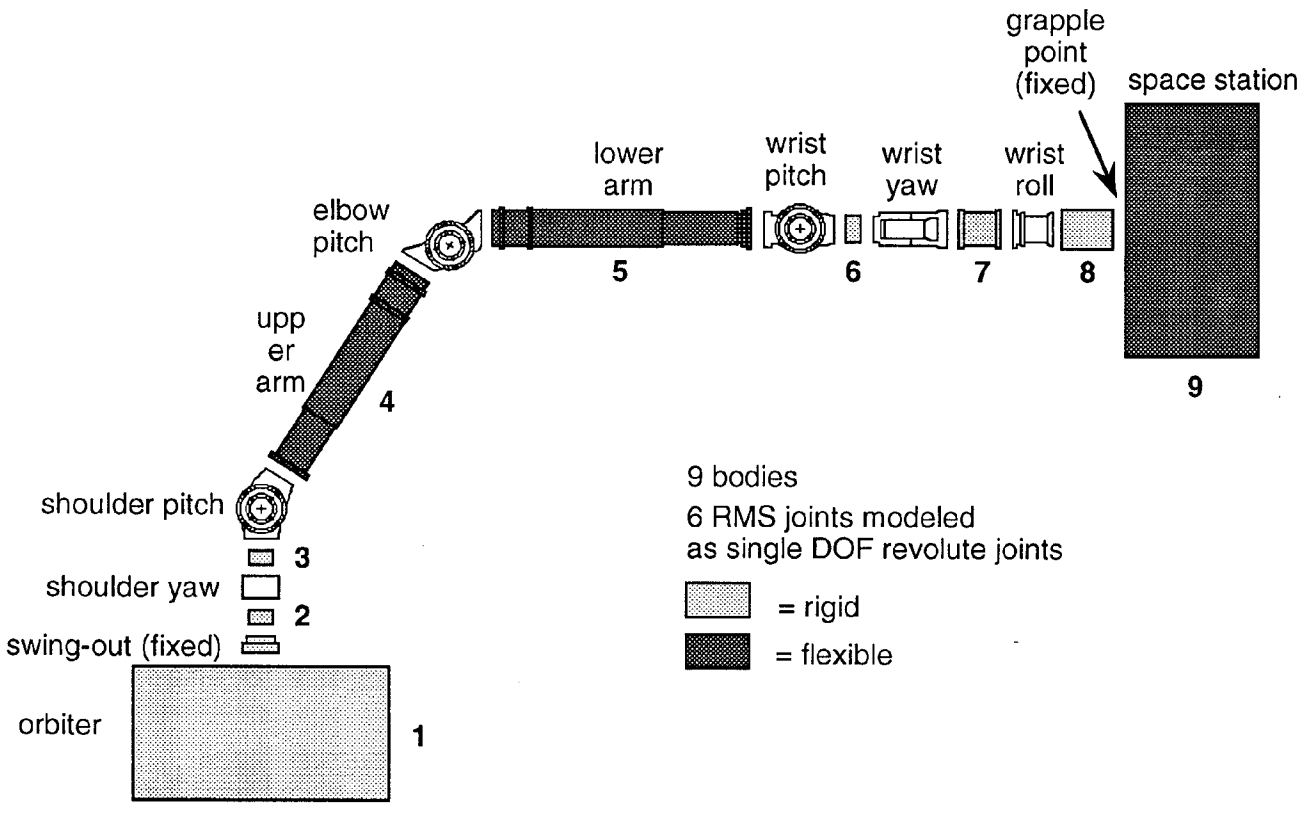

Figure 9 Multi-body representation

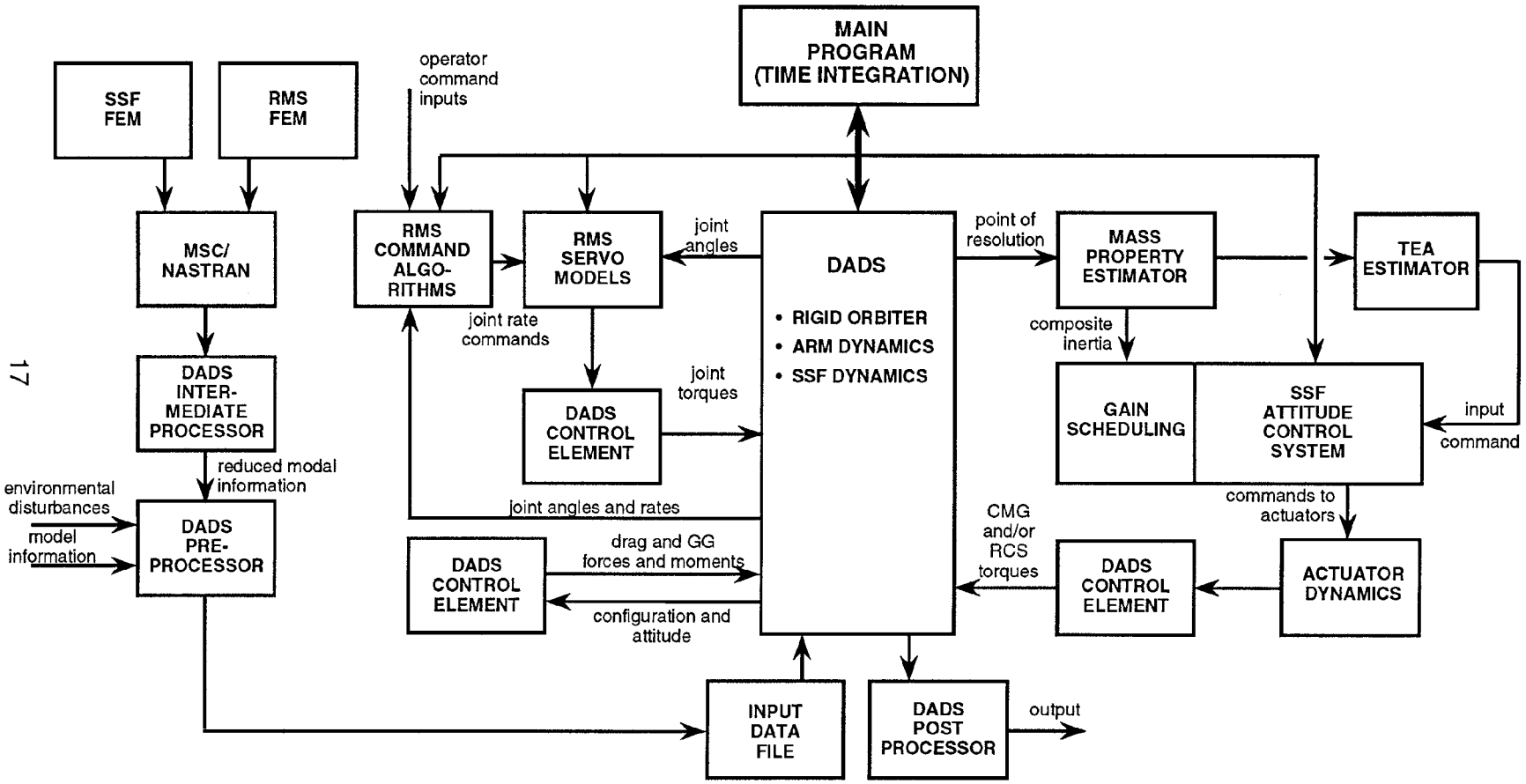

Figure 10 Simulation architecture

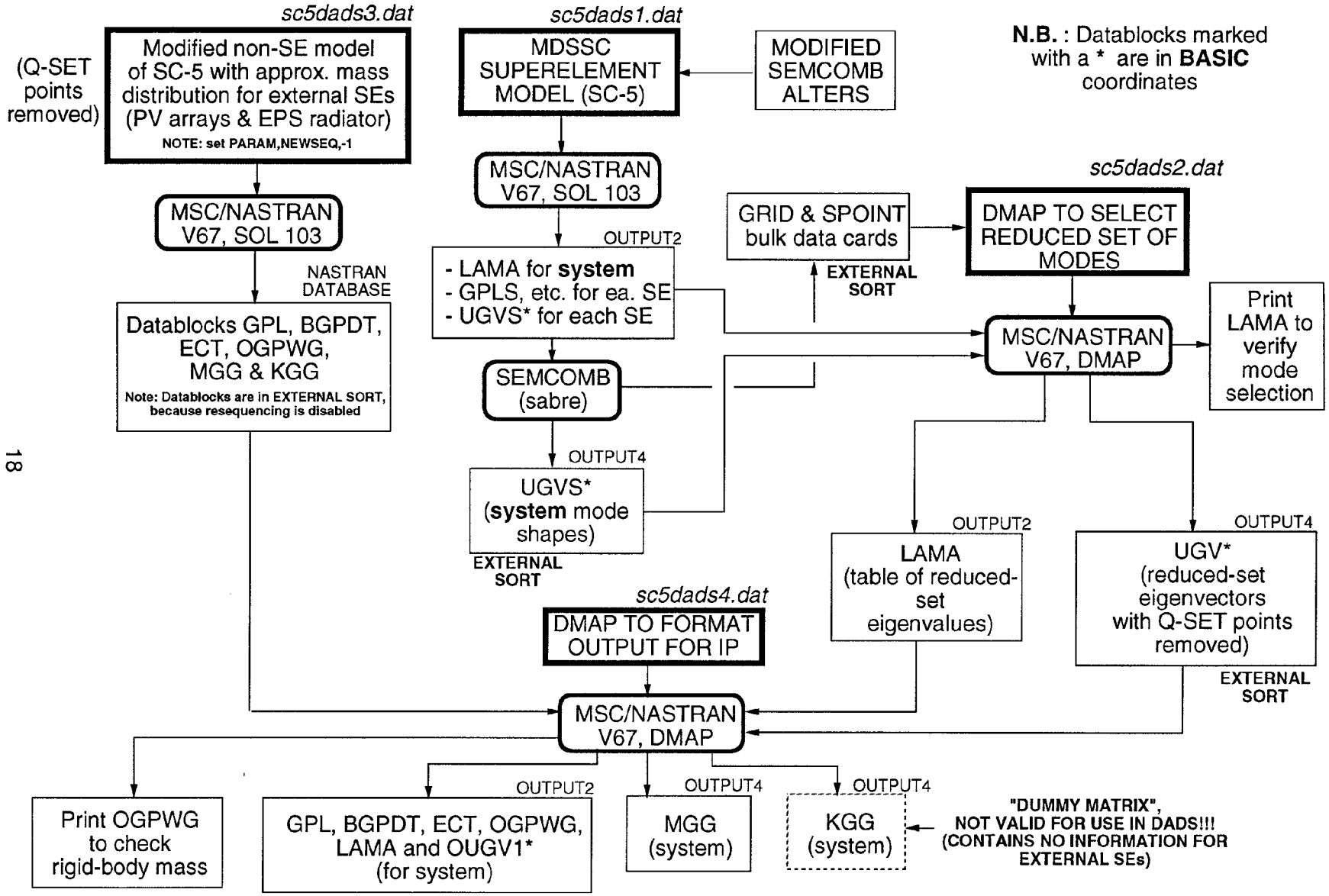

Figure 11 Modified procedure for incorporating SC-5 as a flexible body in DADS simulations

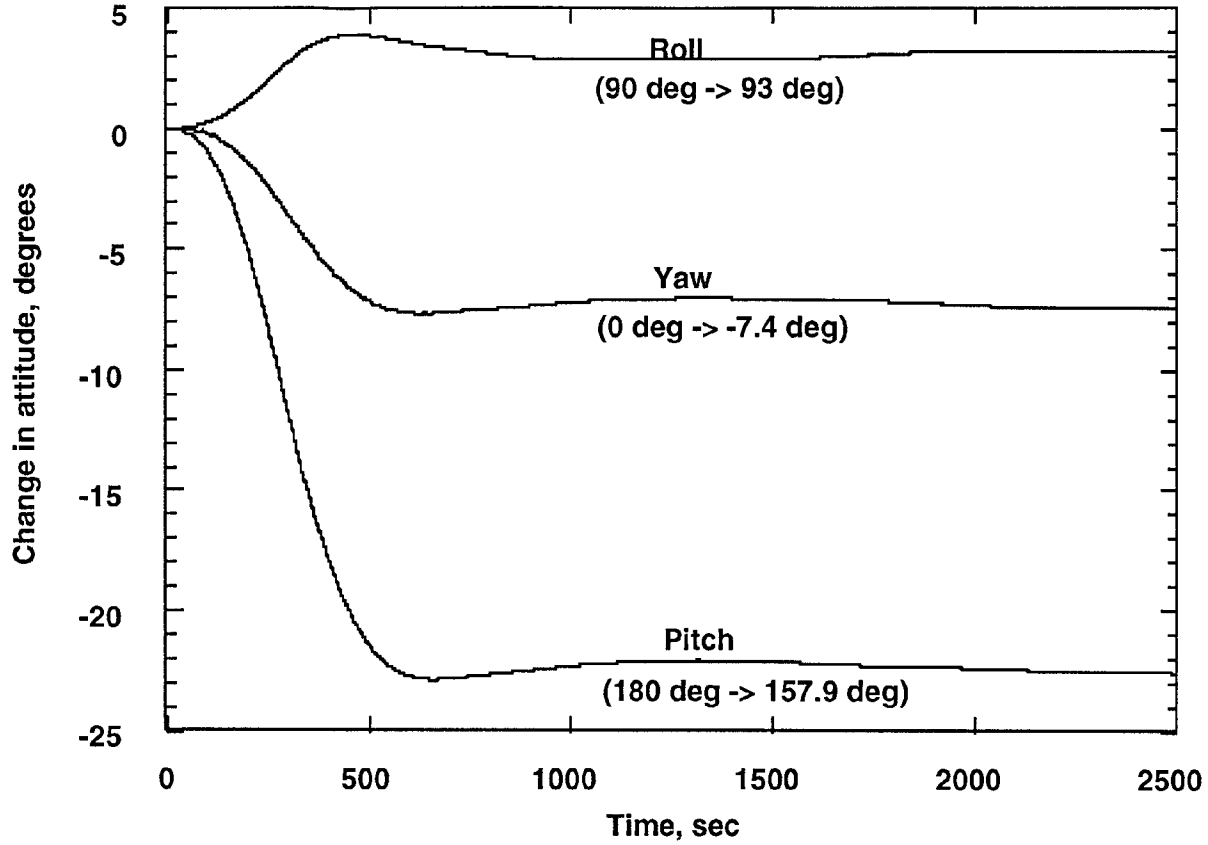

Figure 12 Attitude change during TEA maneuver

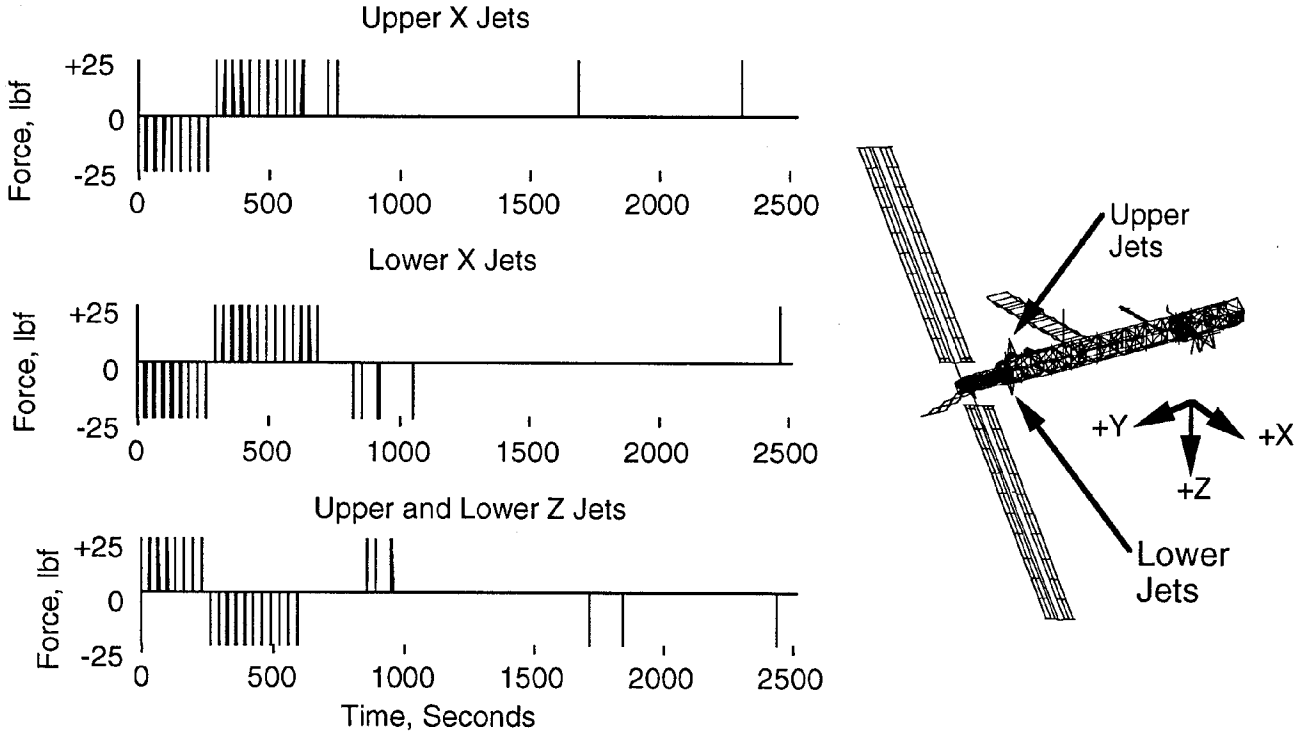

Figure 13 RCS jet firings during TEA maneuver

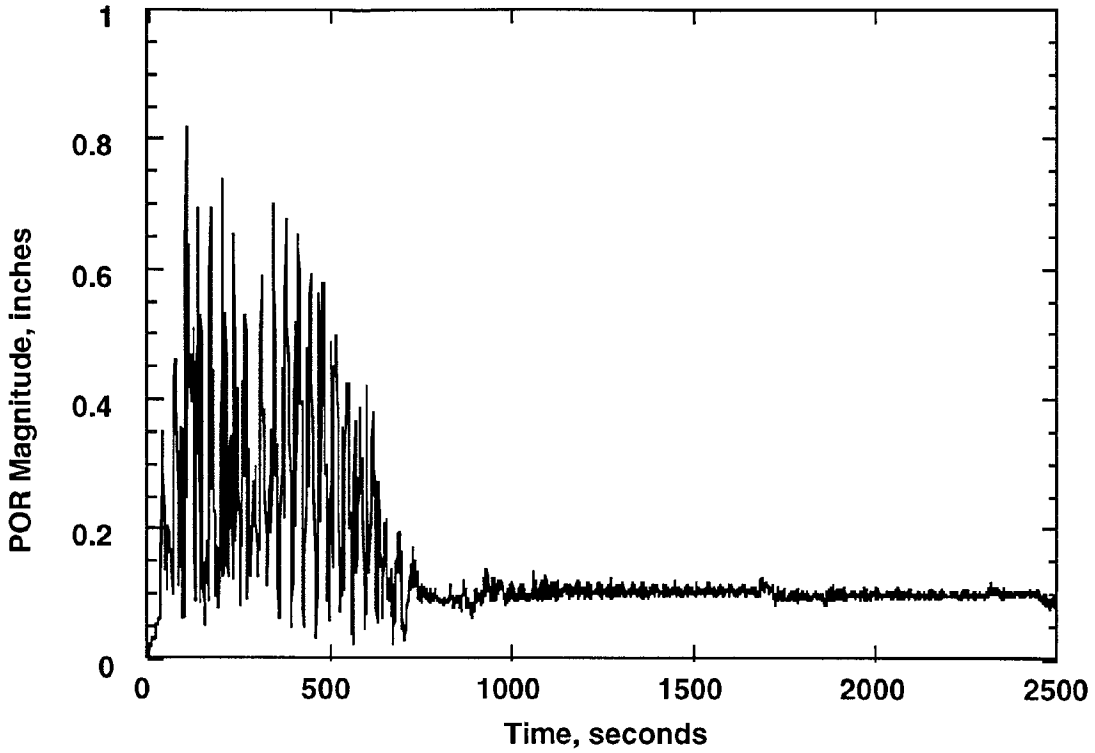

Figure 14 Change in POR magnitude during TEA maneuver

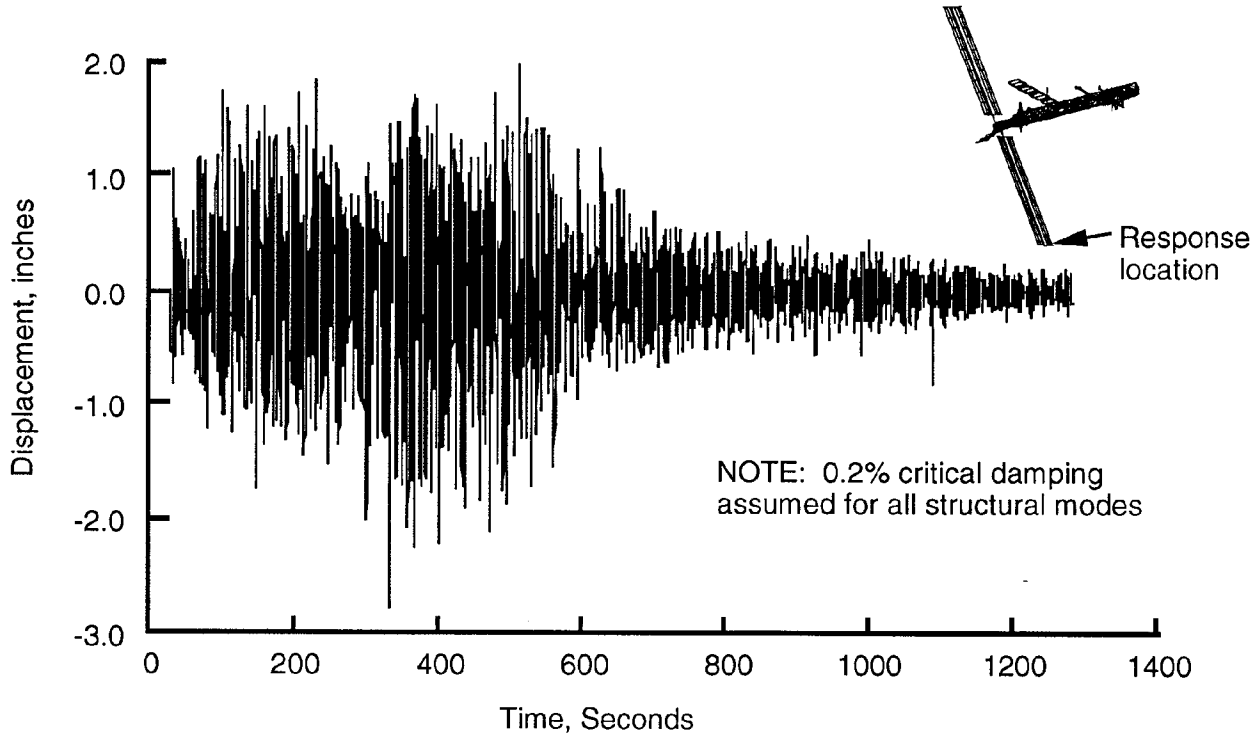

Figure 15 Flexible out-of-plane response of tip of PV array during TEA maneuver